



Optimisation of surface residual stresses using ultrasonic-assisted milling for wire-arc additive manufactured Ni alloy components

Lorenz Engelking¹ · Antonia Eissel² · Dirk Schroeppfer¹ · Kai Treutler² · Thomas Kannengiesser¹ · Volker Wesling²

Received: 19 December 2022 / Accepted: 25 March 2023 / Published online: 13 April 2023
© The Author(s) 2023

Abstract

Nickel alloys are cost intensive materials and generally classified as difficult-to-cut material. However, machining of these materials is needed especially in case of alloy 36 (1.3912), which is commonly used in mould construction for the production of fibre-reinforced composites. With regard to repair, modification and manufacturing of such components, additive manufacturing offers significant economic advantages. Nevertheless, subsequent machining steps are needed to achieve the final component contour and defined surface conditions. Dependent on the material and machining process conditions, detrimental tensile residual stresses may be the result on the machined surface, having negative impact on the component performance and safety. In this investigation, machining experiments were carried out on wire arc additive manufactured components made of alloy 36, varying the cutting speed and the feed rate. In addition, the conventional milling process (CM) was compared with a modern, hybrid machining process, the ultrasonic-assisted milling (US). The cutting forces and the surface-near residual stresses were analysed using X-ray diffraction. A significant improvement of the machinability as well as the surface integrity by using the ultrasonic assistance was observed, especially at low cutting speeds. The CM induced mainly tensile residual stresses, the US mainly compressive residual stresses.

Keywords Surface integrity · Ultrasonic-assisted milling · Additive manufacturing · Ni alloy · Alloy 36

Nomenclature

AM	Additive manufacturing
CM	Conventional milling
DoE	Design of Experiments
EDM	Electrical discharge machining
US	Ultrasonic-assisted milling
WAAM	Wire arc additive manufacturing
XRD	X-ray diffraction
F_{res}	Resulting cutting force
f_z	Feed rate
P_{US}	Ultrasonic assistance
Ra	Arithmetic mean roughness
v_c	Cutting speed
σ_1^{rs}	Maximum principal residual stress

1 Introduction

Nickel alloys are cost intensive and generally classified as difficult-to-cut materials due to their resistance to heat and low thermal conductivity [1]. A typical Ni alloy, alloy 36 (1.3912), was developed in 1897 from Guillaume and stands out for its very low thermal expansion coefficient [2]. It is commonly used for the production of fiber-reinforced composites in the field of mold construction [3]. Additive manufacturing (AM) offers many economic advantages regarding the repair, modification and manufacture of entire components [4]. Subsequent machining of the AM components is mandatory in order to create the required complex structures and final contours. This is usually done using a tool with a geometrically defined cutting edge, such as milling [5]. Surface integrity, i.e., metallurgical (e.g., microstructure), topological (e.g., surface defects) and mechanical (e.g., residual stresses) factors, plays an important role in terms of safety-relevant components [6]. In the course of subsequent machining, however, residual stresses are formed, depending on the cutting conditions. These are due to the thermal and mechanical load of the cutting process [7], resulting in tensile and compressive residual stresses at the surface. Tensile residual stresses are generally undesirable,

✉ Lorenz Engelking
Lorenz.Engelking@bam.de

¹ Bundesanstalt für Materialforschung und -prüfung (BAM),
Unter den Eichen 87, 12205 Berlin, Germany

² Institut für Schweißtechnik und Trennende
Fertigungsverfahren (ISAF), Agricolastraße 2,
38678 Clausthal-Zellerfeld, Germany

as they have a negative influence with regard to fatigue fracture and the propagation and formation of cracks [6, 8]. Compressive residual stresses, on the other hand, have a positive effect in terms of crack propagation control [9], the corrosion resistance and fatigue life [8, 10]. By using hybrid machining processes, such as ultrasonic-assisted milling (US), it is possible to reduce tensile residual stresses compared to conventional milling (CM) or even to generate compressive residual stresses at the surface. In the US process, the milling process is superimposed with a high-frequency oscillation. Rinck et al. have observed a reduction of the cutting force for US compared to CM as well as the formation of compressive residual stresses when milling the difficult-to-cut alloy Ti-6Al-4V with ultrasonic-assistance [11]. Similar results were obtained by Schroepfer et al. when finish milling a difficult-to-cut NiCrCo alloy (IN725) by using a ball end mill. They found that the US process causes lower cutting forces and residual stresses compared to the CM process [5].

In the present work, the influences of subsequent machining by conventional and ultrasonic-assisted milling on the surface integrity and the machining conditions of additive manufactured alloy 36 samples were investigated. The focus was the analysis of the subsurface residual stresses. Two main aspects, firstly the reduction of cutting forces and secondly the reduction of the residual stress state due to ultrasonic-assisted milling are shown. For this purpose, investigations on the quantitative influence of the cutting parameters on the cutting forces as well as the surface integrity were examined by using a Design of Experiments (DoE) for the milling tests.

2 Experimental

Machining tests were carried out on wire arc additive manufactured (WAAM) NILO Filler Metal CF36 in order to investigate the influence of ultrasonic assistance, cutting speed and feed rate on the cutting force as well as the subsurface residual stresses. This material is used as a filler metal for welding alloy 36 and has similar low thermal expansion characteristics [12]. The chemical composition of NILO Filler Metal CF36 is shown Table 1. The parameters of the welding process are presented in Table 2. The WAAM ingot (dimension approx. 120 x 50 x 20 mm³) was welded onto a substrate plate made of alloy 36 to avoid segregation. Subsequently, the specimens for the machining tests were fabricated by electrical discharge machining (EDM) with dimensions of approx. 15 x 15 x 2 mm³ (length x width x height), cf. Fig. 1b.

The finishing milling experiments were carried out without a cutting fluid (under dry conditions) on a 5-axis DMU

Table 1 Chemical composition in wt.-% according to manufacturer [12]

	Fe	Ni	Nb	Mn	C
Balance	36	1.6	0.4	0.2	

Table 2 Welding parameters

Shielding gas	Wire feed [m/min]	Velocity [cm/min]	Wire diameter [mm]	Interlayer temperature [°C]
82% Ar / 18% CO ₂	4.5	30	1.14	120

65 machining center (by DMG MORI) modified for ultrasonic-assisted milling. Down milling mode was used as the milling strategy. The feed direction was in the x-direction (perpendicular to the building direction), cf. Fig. 1a and b. The tool used was a PVD-coated (TiAlSiN) solid carbide ball end mill, with a diameter of 6 mm and four flutes, manufactured by WOLF Werkzeugtechnik GmbH, cf. Fig. 2. For the experiments, the tool was tilted in the primary (x-direction) and in the secondary feed direction (y-direction) by 45°, cf. Fig. 1a and Table 3, based on the findings of [13]. Besides the ultrasonic assistance P_{US} , the parameters cutting speed v_c and feed rate f_z were varied within a DoE in the range recommended by the tool manufacturer, cf. Table 4. This enables the statistical evaluation of the effects and interactions of these factors on the cutting force and the residual stresses.

In addition to the analysis of the cutting forces and the residual stresses, which are described in the following section, surface analyses of the finish-milled specimens were conducted. The arithmetic mean roughness Ra was measured in the y-direction (normal to the feed (x-) direction, cf. Fig. 1a) using a contact profilometer tester (HOMMEL-ETAMIC T1000 by JENOPTIK) in accordance with DIN EN ISO 4287 [14]. In addition, images of the surfaces of two samples were taken using a light microscope (VHX-7000 by KEYENCE).

2.1 Cutting force analysis

The machining forces occurring in the x- (feed force F_f), y- (feed normal force F_{fN}) and z-directions (passive force F_p), cf. Fig. 1a, were measured during the finish milling experiments using a dynamometer (by Kistler, time resolution: 0.1 ms). The resulting cutting force F_{res} was calculated according to equation 1:

$$F_{res} = \sqrt{F_f^2 + F_{fN}^2 + F_p^2} \quad (1)$$

2.2 Residual stresses analysis

The residual stresses were analysed with X-ray diffraction (XRD) using a Goniometer G3 (by Stresstech) and $\sin^2\psi$ method, cf. Table 5, to determine the effect of the cutting conditions. The analysis was performed in each specimen

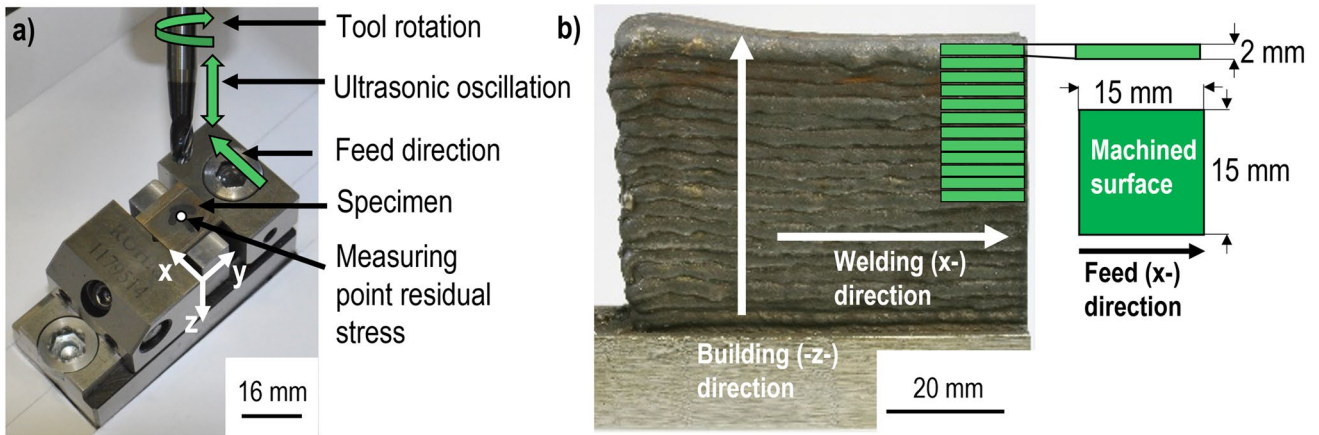


Fig. 1 (a) Experimental setup; (b) the sampling and the specimen dimensions

Fig. 2 Tool geometry of the ball end mill used for the milling experiments

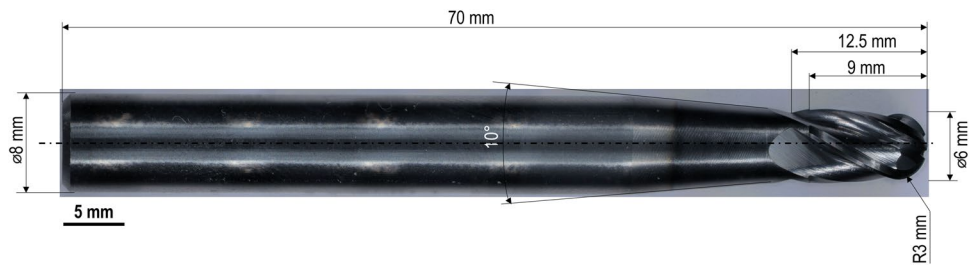


Table 3 Experimental boundary conditions

Angle in x-direction $\lambda = 45^\circ$	Step over $a_p = 0.3 \text{ mm}$	Ultrasonic frequency $F_{US} = 38.7 \pm 0.3 \text{ kHz}$
Angle in y-direction $\tau = 45^\circ$	Cutting engagement $a_e = 0.3 \text{ mm}$	Down milling

center 0° , 45° and 90° to the x-direction (feed direction), cf. Fig. 1a and b. In addition, the residual stress was measured in the as-welded state 0° , 45° and 90° to the welding direction, cf. Fig. 1b. Penetration depth was approx. $5 \mu\text{m}$. The calculations of the residual stresses were performed

using the elastic moduli for alloy 36 (Poisson’s ratio $\nu = 0.25$; Young’s modulus $E = 140 \text{ GPa}$) [15]. Then the maximum principal residual stresses σ_1^{rs} were calculated according to [5].

3 Results

3.1 Machining experiments

The measured cutting forces F_f , F_{fN} and F_p as well as the calculated resulting cutting force F_{res} are exemplarily

Table 4 Experimental data

Test no.	1	2	3	4	5	6	7	8	9	10	11	12
Cutting speed v_c [m/min]	70	30	110	30	70	110	30	110	70	110	30	70
Feed rate f_z [mm/tooth]	0.055	0.04	0.04	0.07	0.055	0.04	0.04	0.07	0.055	0.07	0.07	0.055
Ultrasonic-assistance P_{US} [%]	0	100	0	0	100	100	0	100	100	0	100	0

Table 5 Parameters for XRD residual stress analysis

Measuring mode	Radiation	Detector	Diffraction line	2θ angle
$\sin^2\psi$	Mn-K α	Linear solid-state	(311)	152.3°
Collimator	Tube power	ψ -tilting	ψ -step	Exposure time
3 mm	30 kV/6.7 mA	0° bis $\pm 45^\circ$	9	3 s

shown in Fig. 3 for one milling line and one tool revolution. The maxima and minima of the plots represent one cutting operation each. The different heights of the maxima and minima are due to minor geometry deviations in the course of the manufacturing process of the milling cutters [16].

Figure 4 shows the effect of the cutting speed (4a) and the feed rate (4b) on the resulting cutting force. Furthermore, the US is compared with the CM process. All three factors have a significant influence. In accordance to Gaike et al., the resulting cutting force decreases for both processes by increasing the cutting speed from 30 m/min to 110 m/min [17], cf. Fig. 4a. Furthermore, by increasing the feed rate from 0.04 mm/tooth to 0.07 mm/tooth, the resulting cutting force for both milling processes increases as well (cf. Fig. 4b), which is due to an enhanced material removal in the course of the cutting engagement [17]. Compared to CM, the US process leads to significantly lower cutting forces. This result agrees with the findings of other authors [5, 11, 18, 19]. As Rinck et al. discussed, this effect can be traced back on interrupted cutting process due to the ultrasonic oscillation and the resulting reduced friction between tool and workpiece due to their relative movement [11]. In particular, this observation applies to low cutting speeds and feed rates. If the cutting speed is

increased, the number of oscillations per tool engagement decreases and, thus, the cutting forces of CM and US process converge [19].

3.2 Residual stresses

Figure 5 shows the influence of the cutting speed and the feed rate of both processes on the maximum principal residual stress σ_1^{rs} . Please note, that the penetration depth by XRD for this material and the given tube power is approx. 5 μm and decreases with increasing inclination angle. The XRD analysis system allows a depth correction for the measurement of the stress profile considering high stress gradients in the depth (z-direction) due to the measurement results of the different inclination angles and the depth information [5]. In the as-welded state, the maximum principal residual stress has a value of approx. 102.7 ± 80.1 MPa. Due to the removal of the specimen from the component, most of the residual stress has already been relieved. The remaining tensile residual stresses are due to the high thermal load during the welding process. The ultrasonic assistance exhibits a significant influence within the DoE. The maximum principal residual stresses of the CM process are predominantly tensile residual stresses, cf. Fig. 5a, and US causes mostly compressive residual stresses, cf. Fig. 5b. Rinck et al. attributed this

Fig. 3 Exemplary representation of the cutting forces F_f , F_{fN} and F_p as well as the resulting cutting force F_{res} during milling: (a) one milling line; (b) one tool revolution of test no. 4

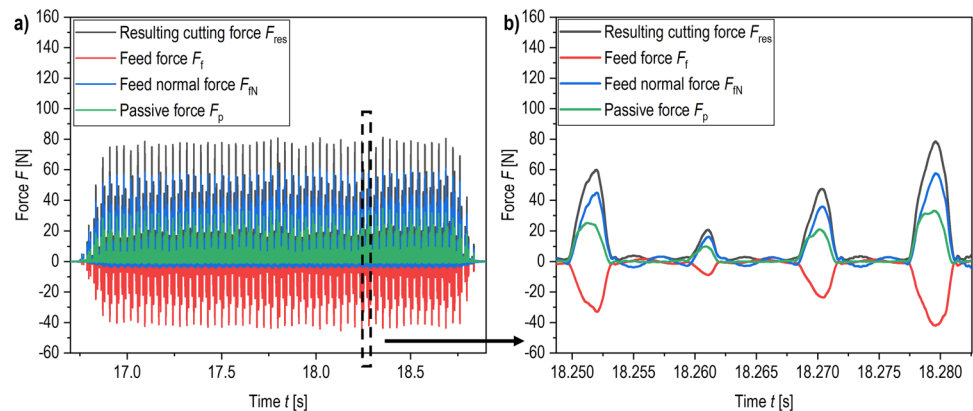
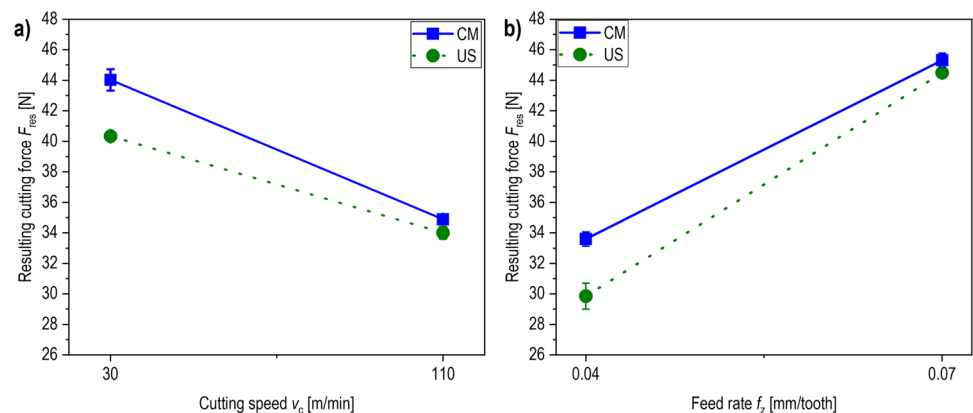


Fig. 4 Resulting cutting force F_{res} versus (a) cutting speed v_c and (b) feed rate f_z



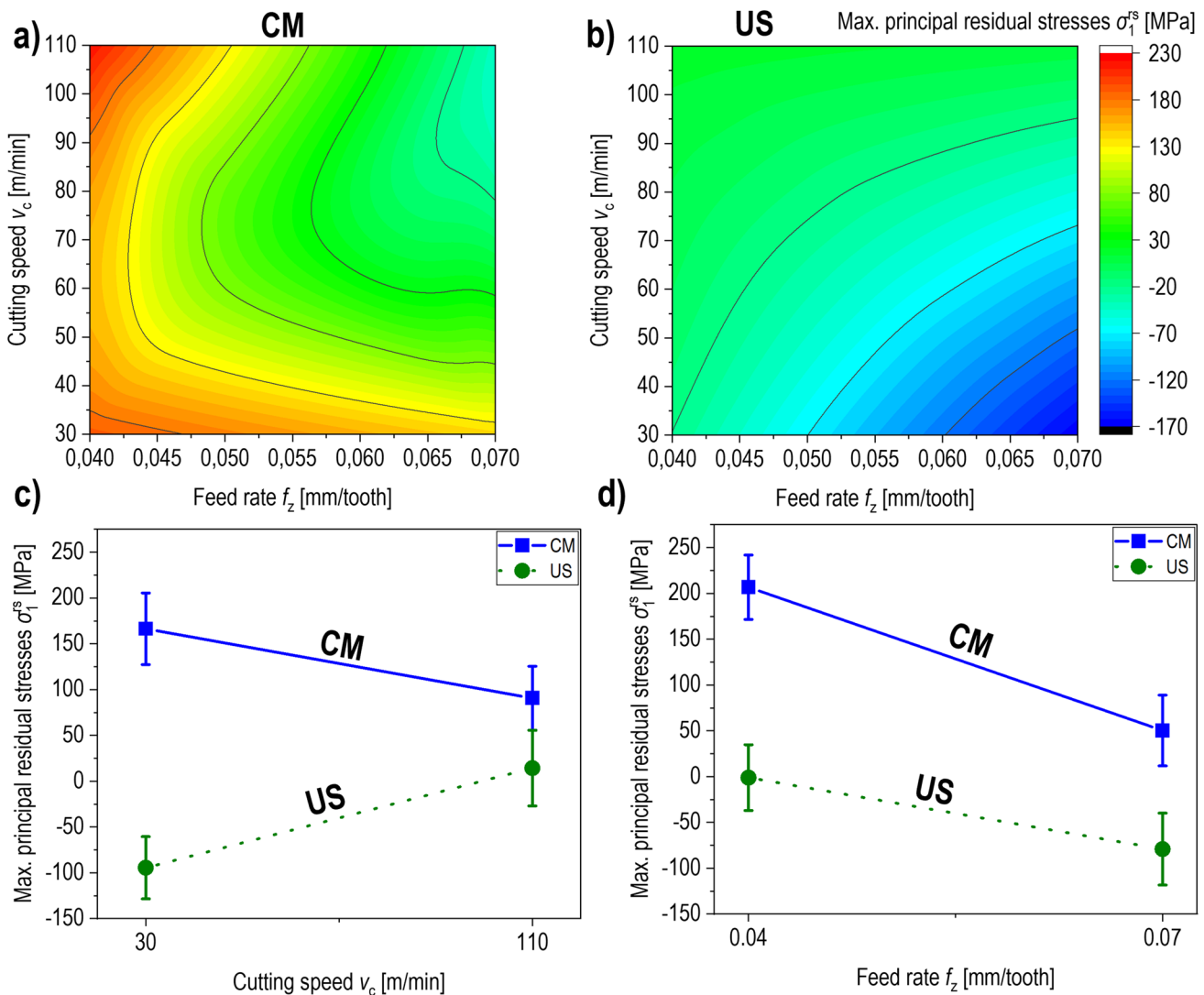


Fig. 5 Maximum principal residual stresses σ_1^{rs} versus cutting speed v_c and feed rate f_z (a) of CM and (b) of US; maximum principal residual stresses σ_1^{rs} versus (c) cutting speed v_c and (d) feed rate f_z

observation to an effect similar to shot peening caused by the axial oscillation of the tool [11]. When considering the CM process, a cutting speed of 110 m/min combined with a feed rate of 0.04 mm/tooth leads to the highest maximum principal residual stress of approx. 222 ± 36 MPa, cf. Fig. 5a. The lowest maximum principal residual stress – even compressive values – are obtained at higher cutting speeds and feed rates for the CM process down to approx. -40 ± 34 MPa. This is due to the higher volume of the chips generated during the milling process compared to the tests with lower feed rate. With a simultaneous increase in cutting speed, more heat can be dissipated into the chips during chip formation, so that overall, the thermal stress during milling for the generated surface and thus possible sources for the formation of tensile residual stresses are reduced. Comparable results have already been observed for other Ni alloys, such as alloy 718 [20].

In accordance to Schroepfer et al., in the present machining tests the US causes significantly lower residual stresses compared to the CM [5], cf. Fig. 5b. The lower the cutting speed and the higher the feed rate, the lower the maximum principal residual stress. Predominantly compressive residual stresses are induced. The lowest principal residual stresses are obtained by the parameter combination $v_c = 30$ m/min and $f_z = 0.07$ mm/tooth with approx. -168 ± 33 MPa. The highest principal residual stresses of the US with a value of approx. 18 ± 37 MPa are resulting from a cutting speed of 110 m/min and a feed rate of 0.04 mm/tooth.

An increasing feed rate from 0.04 mm/tooth to 0.07 mm/tooth causes a considerable reduction of the maximum principal residual stresses for both processes, whereas the residual stresses in US are significantly lower compared to CM, cf. Fig. 5d. This also applies for cutting speed at CM

process. However, as discussed above for the cutting forces, the lower number of oscillations per cutting engagement in the case of increasing the cutting speed in the US process leads to a reduction in efficiency for a given US frequency and amplitude leading to a residual stress state at the surface similar to the CM process. The effect of the ultrasonic assistance is in accordance to the results of the cutting forces, cf. Fig. 5c and d and Fig. 4a and b.

To further consider the correlation between cutting forces and residual stresses on the surface, Hence, Fig. 6 shows the maximum principal residual stresses as a function of the passive force F_p for a) CM and b) US. Both processes exhibit a trend with respect to a reduction of the maximum principal residual stresses with increasing passive force F_p . It is assumed that the passive force acting in the direction of the specimen thickness (z) contributes a high proportion to the residual compressive stresses near the surface due to mechanical compressive loads during chip removal. It can be observed that the passive force shows similarly high values for both processes US and CM. Overall, however, significantly lower residual stresses or compressive residual stresses are already generated on the surface at lower passive forces.

3.3 Surface quality

The comparison of the surface finish is shown in Fig. 7. The analysis of the arithmetic mean roughness Ra vs. cutting speed, cf. Fig. 7a, shows a similar behavior for CM and US as observed for the maximum principal residual stress, cf. Fig. 5c. With increasing cutting speed, Ra of the CM decreases, whereas an increase is observed for US. The lowest roughness of all tests is achieved by low cutting speed for US process. Fig. 7b and c show the finish milled surface of the tests with the lowest residual stresses each for CM and US process (Fig. 7b test no. 10, $\sigma_1^{rs} = -40 \pm 34$ MPa, CM; Fig. 7c test no. 11, $\sigma_1^{rs} = -168 \pm 33$ MPa, US). The surface of test no. 11 exhibits a significantly lower number of insufficient surface areas in the form of local material accumulations and decomposition which appear black in the pictures compared to the surface of test no. 10, which is also reflected in the lower arithmetic mean roughness $Ra = 0.79 \mu\text{m}$ (US) compared to $Ra = 1.02 \mu\text{m}$ (CM). Consequently, the US process with a cutting speed of 30 m/min and a feed rate of 0.07 mm/tooth implies the highest surface quality of all parameter combinations investigated.

Fig. 6 Maximum principal residual stresses σ_1^{rs} versus passive force F_p for (a) CM and (b) US

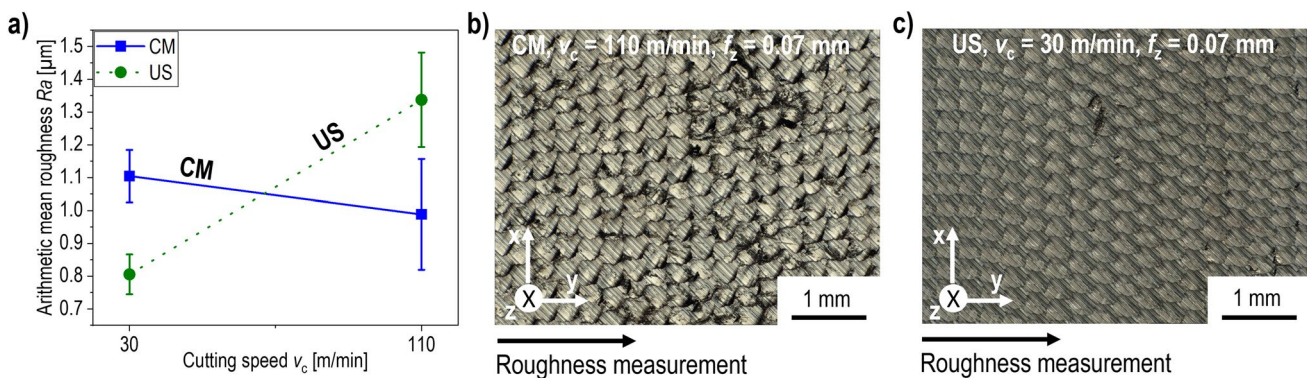
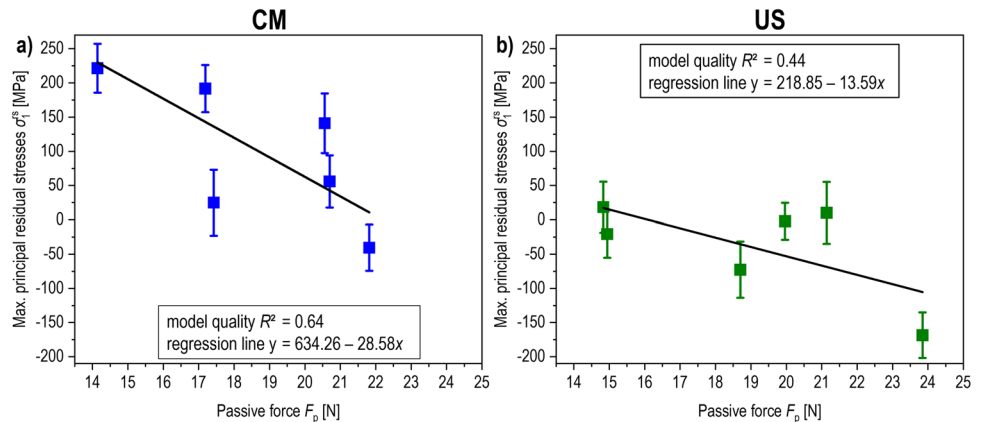


Fig. 7 (a) Arithmetic mean roughness Ra vs. cutting speed v_c ; (b) the surface of test no. 10 and (c) of test no. 11

4 Discussion

The results of the study show a positive influence of the ultrasonic assistance on the machinability as well as the surface integrity when machining AM components made of alloy 36. US causes significantly lower cutting forces compared to the CM process, which can be attributed to the reduced friction between the workpiece and the milling tool and the interrupted cutting process due to the axial oscillation of the milling tool, which overlays the kinematics of the CM process [11]. At a cutting speed of 30 m/min, a four-flute ball nose end mill and an ultrasonic frequency of 40 kHz, the result are approx. 377 tool oscillations per cutting engagement. The reduced cutting force is in accordance with the results of other authors who have also investigated the influence of ultrasonic assistance in machining difficult-to-cut materials [5, 11, 18]. In addition, the US process has been shown to significantly reduce the residual stress state compared to CM, which has also been noted in recent studies [5, 11]. The compressive residual stresses induced by US have a positive effect on fatigue strength and resistance to stress corrosion cracking [8]. For the first time, a correlation between the passive force F_p and the subsurface maximum principal residual stresses was analysed in this study. Thereby, the trend for both US and CM with regard to a lower maximum principal residual stress at the surface with a higher passive force F_p of the finish-milled AM components is evident, but the model quality is not particularly high with $R^2 = 0.64$ and 0.44 , respectively. To verify this relationship between the passive force F_p and the residual stress, more extensive investigations are necessary. It is suggested to investigate other materials for which an effect on the reduction of the residual stress state by using ultrasonic assistance has already been demonstrated, such as Ti-6Al-4V or IN725 [5, 11]. Please note that in this study the cutting samples of the AM components were machined solely perpendicular to the building direction. Thus, the analysed residual stresses solely represent the plane stress state perpendicular to the building direction. Due to the naturally high anisotropy of AM components, the investigation of the microstructural anisotropy is an essential necessity in order to finally classify and evaluate the results obtained in this study. Lizzul et al. have shown, for example, that the microstructural anisotropy of AM components has an influence on the resulting surface integrity of the subsequent machining process [21]. Furthermore, an enormous additive manufacturing-induced anisotropy of the tool wear was shown [22], which is why it can be assumed that the cutting force also shows a strong additive manufacturing-induced anisotropy when machining AM components. In addition, a detailed comparison of the tool wear of the CM process with the US process is recommended, as an increase in the tool life due to the ultrasonic assistance was observed, for example, by Liu et al. [23]. Further potentials

result from chip analyses analogous to [18, 24]. The reduced roughness of the finish milled surfaces shown in this study, especially at low cutting speeds, is also in accordance with the results obtained in previous investigations [11, 18]. One explanation for the reduced roughness is the lower amount of feed marks due to the ultrasonic assistance [11]. Furthermore, the low roughness and defect density at a cutting speed of 30 m/min can be explained by the avoidance of the formation of a built-up edge, as the ultrasonic oscillation of the tool presumably reduces the adhesion of the material to the tool cutting edge and consequently prevents the formation of a built-up edge. Reduced adhesion was already found by Koshimizu for ultrasonic-assisted turning of Ti-6Al-4V [25]. The observed increased surface integrity in terms of lower number of insufficient surface areas, reduced roughness and a lower residual stress state has a positive influence on the service life, safety and component performance in use [5, 26, 27]. An analysis of the boundary zone of the finish milled surfaces to investigate the microstructural influence of the machining process is necessary for a complete evaluation of the surface integrity, analogously to Schroepfer et al. [5]. The experiments carried out in this study were done solely under dry conditions. An analysis with different cooling strategies during finish milling should therefore be considered in future investigations, as these also have an influence on the resulting surface integrity [28].

5 Summary and Conclusion

Investigations were carried out to analyse the influence of the milling parameters cutting speed and feed rate as well as ultrasonic assistance on AM components of alloy 36 on the surface integrity and machining conditions. The following results were obtained:

- (1) US process causes significantly lower resulting cutting forces compared to CM, especially at low cutting speeds and feed rates.
- (2) CM process induces primarily subsurface tensile residual stresses, while US process induces primarily compressive residual stresses, which have a positive effect on the component performance in service. The effect of ultrasonic assistance is highest at low cutting speeds analogous to the results of cutting force.
- (3) Higher feed rates generate lower residual stresses at the surface within the experimental matrix.
- (4) As the passive force increases, both machining processes tend to generate lower maximum principal residual stresses.
- (5) The highest surface integrity in terms of roughness, topography and residual stresses is achieved with low cutting speed $v_c = 30$ m/min, a high feed rate $f_z = 0.07$ mm/tooth and ultrasonic assistance.

Author Contributions All authors contributed to the study conception and design. Material preparation, data collection and analysis were performed by Lorenz Engelking and Antonia Eissel. The first draft of the manuscript was written by Lorenz Engelking and Antonia Eissel and all authors commented on previous versions of the manuscript. All authors read and approved the final manuscript.

Funding Open Access funding enabled and organized by Projekt DEAL. The IGF project IGF No. 20.979 N (DVS 01.3211) of the Research Association of the DVS was supported by the Federal Ministry for Economic Affairs and Climate Action by the AiF as part of the program for support of the cooperative industrial research (IGF) on the basis of a decision by the German Bundestag. We would like to thank for this funding and the companies involved in the project committee for their support, in particular WOLF Werkzeugtechnologie GmbH for providing the milling tools. We also thank Andreas Boerner from the BAM for his support in the milling experiments.

Declarations

Conflict of interest The authors declare no competing interests.

Open Access This article is licensed under a Creative Commons Attribution 4.0 International License, which permits use, sharing, adaptation, distribution and reproduction in any medium or format, as long as you give appropriate credit to the original author(s) and the source, provide a link to the Creative Commons licence, and indicate if changes were made. The images or other third party material in this article are included in the article's Creative Commons licence, unless indicated otherwise in a credit line to the material. If material is not included in the article's Creative Commons licence and your intended use is not permitted by statutory regulation or exceeds the permitted use, you will need to obtain permission directly from the copyright holder. To view a copy of this licence, visit <http://creativecommons.org/licenses/by/4.0/>.

References

- Karaguzel U, Olgun U, Uysal E, Budak E, Bakkal M (2014) Increasing tool life in machining of difficult-to-cut materials using nonconventional turning processes. *Int J Adv Manuf Technol* 77(9–12):1993–2004
- Sahoo A, Medicherla VRR (2021) Fe-Ni Invar alloys: A review. *Mater Today: Proc* 43:2242–2244
- Seeger M (2013) Entwicklung und Bewertung lichtbogengespritzter Invar-Laminier Vorrichtungen für die CFK Produktion. Fakultät für Maschinenwesen Technische Universität München
- Treutler K, Wesling V (2021) The Current State of Research of Wire Arc Additive Manufacturing (WAAM): A Review. *Appl Sci* 11(18)
- Schroepfer D, Treutler K, Boerner A, Gustus R, Kannengiesser T, Wesling V, Maus-Friedrichs W (2021) Surface finishing of hard-to-machine cladding alloys for highly stressed components. *Int J Adv Manuf Technol* 114(5–6):1427–1442
- Ulutan D, Ozel T (2011) Machining induced surface integrity in titanium and nickel alloys: A review. *Int J Mach Tool Manuf* 51(3):250–280
- Ma Y, Feng P, Zhang J, Wu Z, Yu D (2016) Prediction of surface residual stress after end milling based on cutting force and temperature. *J Mater Process Technol* 235:41–48
- Masmiati N, Sarhan AAD, Hassan MAN, Hamdi M (2016) Optimization of cutting conditions for minimum residual stress, cutting force and surface roughness in end milling of S50C medium carbon steel. *Measurement* 86:253–265
- Salvati E, Zhang H, Fong KS, Song X, Korsunsky AM (2017) Separating plasticity-induced closure and residual stress contributions to fatigue crack retardation following an overload. *J Mech Phys Solids* 98:222–235
- Mirkoochi E, Bocchini P, Liang SY (2019) Inverse analysis of residual stress in orthogonal cutting. *J Manuf Process* 38:462–471
- Rinck PM, Gueray A, Kleinwort R, Zaeh MF (2020) Experimental investigations on longitudinal-torsional vibration-assisted milling of Ti-6Al-4V. *Int J Adv Manuf Technol* 108(11–12):3607–3618
- S.M.W.P. Company, Nickel Alloy Welding Product Catalogue., (2009).
- Slătineanu L, Wojciechowski S, Maruda RW, Królczyk GM, Nagit G, Dodun O, Merticaru V, Coteata M, Ripanu MI, Mihalache AM, Boca M, Ibanescu R, Panait CE, Oancea G, Kyratsis P (2017) The application of response surface method to optimization of precision ball end milling. *MATEC Web Conf* 112:01004
- DIN EN ISO 4287.
- S.M. Corporation, The NILO® and NILOMAG® Nickel-Iron Alloys, Publication Number SMC-031 (2004).
- Richter T, Schröpfer D, Rhode M, Börner A (2020) Influence of modern machining processes on the surface integrity of high-entropy alloys. *IOP Conf Ser: Mater Sci Eng* 882:012016
- Gaikhe V, Sahu J, Pawade R (2018) Optimization of Cutting Parameters for Cutting Force Minimization in Helical Ball End Milling of Inconel 718 by Using Genetic Algorithm. *Procedia CIRP* 77:477–480
- Ni C, Zhu L, Liu C, Yang Z (2018) Analytical modeling of tool-workpiece contact rate and experimental study in ultrasonic vibration-assisted milling of Ti-6Al-4V. *Int J Mech Sci* 142–143:97–111
- L. Zheng, W. Chen, D. Huo, *Vibration Assisted Machining: Theory, Modelling and Applications*, 2021.
- Wang J, Zhang D, Wu B, Luo M (2017) Residual Stresses Analysis in Ball end Milling of Nickel-Based Superalloy Inconel 718. *Mater Res* 20(6):1681–1689
- Lizzul L, Bertolini R, Ghiotti A, Bruschi S (2020) Effect of AM-induced Anisotropy on the Surface Integrity of Laser Powder Fused Ti6Al4V Machined Parts. *Procedia Manuf* 47:505–510
- Lizzul L, Sorgato M, Bertolini R, Ghiotti A, Bruschi S (2020) Influence of additive manufacturing-induced anisotropy on tool wear in end milling of Ti6Al4V. *Tribol Int* 146:106200
- Liu X-F, Wang W-H, Jiang R-S, Xiong Y-F, Lin K-Y (2020) Tool wear mechanisms in axial ultrasonic vibration assisted milling in-situ TiB2/7050Al metal matrix composites. *Adv Manuf* 8(2):252–264
- Ahmed F, Ko TJ, Kurniawan R, Kwack Y (2021) Machinability analysis of difficult-to-cut material during ultrasonic vibration-assisted ball end milling. *Mater Manuf Processes*:1–12
- Koshimizu S (2008) Ultrasonic Vibration-Assisted Cutting of Titanium Alloy. *Key Eng Mater* 389–390:277–282
- M'Saoubi R, Outeiro JC, Chandrasekaran HO, Dillon OW Jr, Jawahir IS (2008) A review of surface integrity in machining and its impact on functional performance and life of machined products. *Int J Sustain Manuf* 1(1–2):203–236
- Yue C, Gao H, Liu X, Liang S (2018) Part Functionality Alterations Induced by Changes of Surface Integrity in Metal Milling Process: A Review. *Appl Sci* 8(12):2550
- Thakur A, Gangopadhyay S (2016) State-of-the-art in surface integrity in machining of nickel-based super alloys. *Int J Mach Tool Manuf* 100:25–54

Publisher's note Springer Nature remains neutral with regard to jurisdictional claims in published maps and institutional affiliations.